Available online at www.sciencedirect.com

ScienceDirect

Procedia Structural Integrity 23 (2019) 439–444

Structural Integrity Procedia

www.elsevier.com/locate/procedia

9th International Conference on Materials Structure and Micromechanics of Fracture

Thermal cycling behaviour of plasma-sprayed thermal barrier coatings with pre-oxidized NiCrAlY and NiCoCrAlY bond-coats

Karel Slámečka[a,*], David Jech[a], Lenka Klakurková[a], Serhii Tkachenko[a], Michaela Remešová[a], Pavel Gejdoš[a], Ladislav Čelko[a]

[a]*CEITEC – Central European Institute of Technology, Brno University of Technology, Purkyňova 123, 612 00 Brno, Czech Republic*

Abstract

This contribution deals with thermal cycling of thermal barrier coatings (TBCs) with NiCrAlY and NiCoCrAlY bond-coats, and yttria stabilized zirconia (YSZ) top-coat that were prepared by atmospheric plasma spraying from commercial powders. The samples were pre-oxidized, based on isothermal oxidation of the two bond-coats, in order to diminish the influence of residual stresses after spraying on thermal cycling experiments. Surface topographies of both bond-coats were measured using optical profilometry and several surface parameters were evaluated to characterize them. Microstructural degradation caused by thermal cycling was examined by scanning electron microscopy with an emphasis on the role of bond-coat surface features on local damage mechanisms. An important micromechanism for TBCs with the NiCoCrAlY bond-coat was multiple parallel cracking of the TGO layer that was likely also responsible for lower endurance of these coatings.

Keywords: Thermal barrier coatings; Bond-coat; Plasma spray; Roughness; Oxidation; Thermal cycling.

1. Introduction

Plasma-sprayed thermal barrier coatings (TBCs) are multilayer material systems that found their main application within the hot section of land-based and aircraft gas turbines. A typical TBC comprises an upper ceramic layer (yttria-

* Corresponding author. Tel.: +420-541-14-2812; Fax: +420-541-14-2842.
E-mail address: karel.slamecka@ceitec.vutbr.cz

10.1016/j.prostr.2020.01.126

stabilized zirconia – YSZ – is a current industry standard), a bottom metallic bond-coat layer, most often of *M*CrAlY type (*M* = Ni, Co, or Ni + Co), and a gradually developing thermally grown oxide (TGO) layer between them, which is the ultimate cause of failure. The typical local damage micromechanisms include cracking along the YSZ/TGO interface at the peaks and in the surrounding YSZ top-coat, the off-peak YSZ cracking, and delamination of the TGO layer from the bond-coat, see Padture et al. (2002). The purpose of this particular study was to evaluate the thermal cycling endurance of pre-oxidized TBCs with NiCrAlY and NiCoCrAlY bond-coats and to assess damage progression in these coatings.

2. Experimental procedure

2.1. Preparation of samples and furnace thermal cycling

Substrate discs (2.5 cm diameter × 5 mm thick, with 45° × 1 mm edge bevel) were prepared from nickel base superalloy. The discs were grit blasted with Al_2O_3, cleaned in an ultrasonic cleaner and then sprayed with NiCrAlY or NiCoCrAlY bond-coat using a plasma spraying equipment GTV MF-P1000 and a Sulzer Metco F4 MB-XL plasma gun. The composition (in wt.%) of these coatings was Ni-22Cr-10Al-1Y (GTV, 60.46.8 powder) and Ni-23Co-17Cr-12Al-0.5Y (H.C. Stark, Amperit 410). The YSZ layer of ZrO2-8Y2O3 composition (H.C. Stark, Amperit 831) was sprayed as the top coat using the same spray equipment. All coatings were prepared in air and on one face only using plasma spray parameters recommended by powder producers, Tab. 1. One sample per each bond-coat type was left without the YSZ top-coat and subjected to isothermal oxidization at 1050 °C for 100 h in air (LAC, LH06 furnace) to study unconstrained bond-coat oxidation.

Table 1. Plasma spray conditions and resulting coating thicknesses.

Parameter	NiCrAlY	NiCoCrAlY	YSZ
Powder size (μm)	-38/+16	-45/+22	-45/+10
Gun amperage (A)	600	650	500
Primary Ar (slpm)	55	65	30
Secondary H_2 (slpm)	9.5	8	3
Carrier Ar (slpm)	5	2	30
Spray distance (mm)	140	145	130
Traverse speed (mm/s)	150	150	200
Number of passes	3	3	8
Coating thickness (μm)	240 ± 10	170 ± 20	350 ± 10

The two studied bond-coat types have different thicknesses (Tab. 1), which is common in plasma spray technology. It can be assumed that the residual stresses in these coatings are also rather different, not only because of different thicknesses, but also due to different powder material and different spray conditions, see Zhang et al. (2013). In order to diminish the influence of these factors on thermal cycling experiments, the samples with full TBC were pre-oxidized based on the results of oxidation of unconstrained bond-coats. The target thickness of the TGO layer of pre-oxidized samples was chosen to be 3 μm, which corresponds with the onset of stress conversion, *i.e.* local reversal of tensile and compressive stresses at the interface due to the presence of interfacial peaks and valleys, see Vaßen et al. (2001) and Slámečka et al. (2016). It is expected that this procedure somewhat relieves the residual stresses due to the spraying process, see Liu et al. (2013), and it also avoids effects of residual stresses on cyclic damage of the TBC system during the early oxidation stage. Moreover, this procedure shortens the length of tests, thus reducing their cost.

The furnace thermal cycling (FTC) experiments were conducted in modified LAC LT50 tube furnace. The pre-oxidized samples were cycled between room temperature and the temperature of 1050 (2 samples) and 1150 °C (1 sample). Each thermal cycle consisted of 24 min of heating and dwell at the test temperature, and 12 min of air-fan forced cooling outside the furnace. The experiments were interrupted when the YSZ top-coat visually appeared to be delaminated from 75 % of total area or more.

2.2. Characterization methods

Specimens were prepared for microstructural observations using standard metallographic methods, i.e. precise, slow-speed cutting, grinding with abrasive papers and polishing with diamond paste. Optical microscopy (Olympus GX-51) and scanning electron microscopy (SEM; Philips XL30, Tescan Lyra3) together with energy dispersive spectroscopy (EDS) were used for characterization.

The surface roughness of as-sprayed and isothermally oxidized bond-coats was characterized based on optical profilometry measurements (Fries Research & Technology GmbH, Microprof 100). Data were acquired from 2×2 mm^2 regions using the scanning step of 4 μm in both x and y horizontal scanning directions. Residual surface data were obtained by removal of outliers and least square plane removal. These data were described by several common roughness parameters: S_a (arithmetic average roughness), S_q (root mean square roughness), Sk (skewness), K (kurtosis), and R_S (surface roughness, developed area), see Dong et al. (1993), ISO 25178-2 (2012).

3. Results and discussion

3.1. As-sprayed and oxidized NiCrAlY and NiCoCrAlY bond-coats

As-sprayed NiCrAlY coatings were quite compact and, because of relatively small powder particles, contained many internal-oxide stringers that were formed during spraying in air. In comparison, as-sprayed NiCoCrAlY coatings contained fewer oxide stringers but their internal porosity was higher and the pores were larger. The internal microstructure affected the internal oxidation and, therefore, thermal cycling experiments (*cf.* Fig. 3).

The character of the TGO layer developed on each bond-coat was influenced by its chemical composition. In both cases, the TGO layer consisted of a thicker, continuous alumina sub-layer, and a thinner, upper sub-layer of mixed oxides. Small pores were often present near the mixed-oxides/TGO interface, especially for NiCoCrAlY bond-coat, for which the mixed oxide layer was also less regular, Fig. 1. Mixed oxides occasionally appeared also as clusters, which were located at highly irregular interfacial regions and around unmelted/partially-melted powder particles (*cf.* Fig. 3). Similar oxidation behaviour was earlier reported for CoNiCrAlY–YSZ (full TBC) samples in Slámečka et al. (2015).

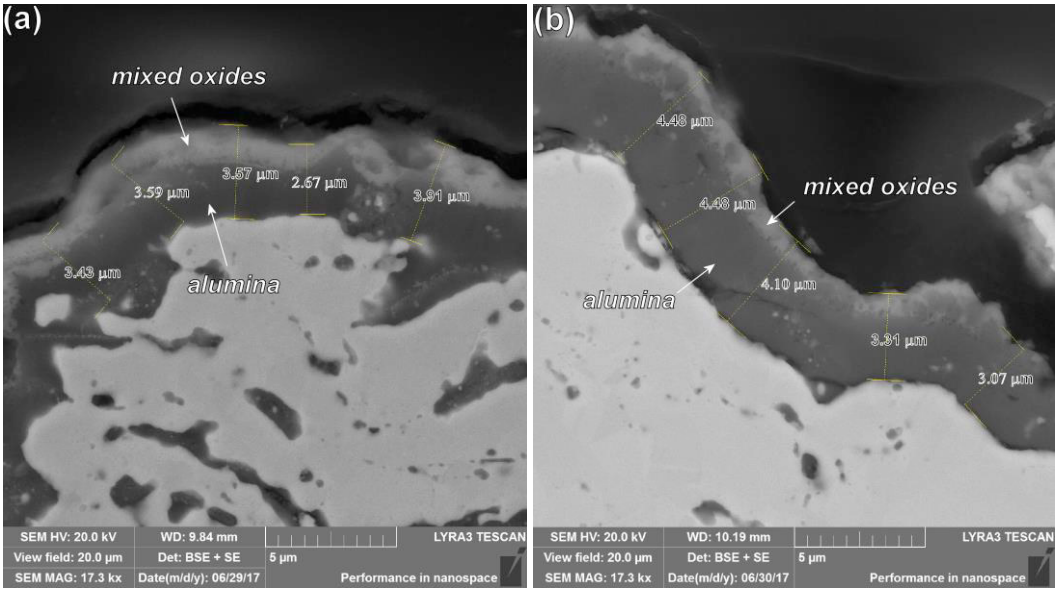

Fig. 1. The TGO layer developed on (a) NiCrAlY and (b) NiCoCrAlY bond-coats after 100 h oxidation at 1050 °C. The dark part is alumina (Al_2O_3), as confirmed by EDS. The outer, brighter layer is composed of mixed oxides.

The thickness of the TGO layer, t_{TGO}, evaluated from fourteen high-resolution micrographs, such as those shown in Fig. 1, was somewhat lower for the NiCrAlY coating (t_{TGO} = 3.1 ± 0.6 μm) than for the NiCoCrAlY coating (t_{TGO} = 3.7 ± 0.8 μm). The thickness of the mixed-oxide layer, where continuous, was estimated to be 1.2 μm on average in both cases. The pre-oxidation of full TBC samples designated for thermal cycling experiments to the chosen target thickness t_{TGO} = 3 μm was based on data related to the full TGO scale. It was assumed that the oxidation process can be described as parabolic and that the initial thickness of the TGO layer after spraying was negligible, *i.e.* $t_{TGO}=k\sqrt{t}$, where t = 100 h and the oxidation rate constant k is thus 0.31 for NiCrAlY and 0.37 μm·h$^{-0.5}$ for NiCoCrAlY coatings, corresponding to pre-oxidation time of 93 and 66 h, respectively.

Some example height maps of as-sprayed and oxidized NiCrAlY and NiCoCrAlY coatings are shown in Fig. 2, revealing the differences between the two states. Generally, the plasma-sprayed surfaces are composed of small-scale (tens of μm) roughness features related to individual powder particles and large-scale (hundreds of μm) waviness features which are likely related to the plasma-spray process itself, see Skalka et al. (2015). Oxidation, as expected, proceeds on the roughness scale and is accelerated near partially melted particles and torturous interface regions, Fig. 2. The calculated roughness parameters are reported in Tab. 2. The results show that the vertical extend (S_a and S_q) of NiCrAlY coatings was less than that of NiCoCrAlY coatings (Fig. 2), which can be related to different powder size (Tab. 1), as experimentally exploited in several previous studies, see Vaßen et al. (2001) and Eriksson et al. (2013). Skewness *Sk* and kurtosis *K* were found to be slightly positive (0.0-0.3). None of these reported features distinctly changed after oxidation. Nevertheless, the surface roughness R_S, which represents the area of a coating and unlike the previous parameters reflects also the spatial relationships, is notably smaller for oxidized samples, suggesting surface smoothing.

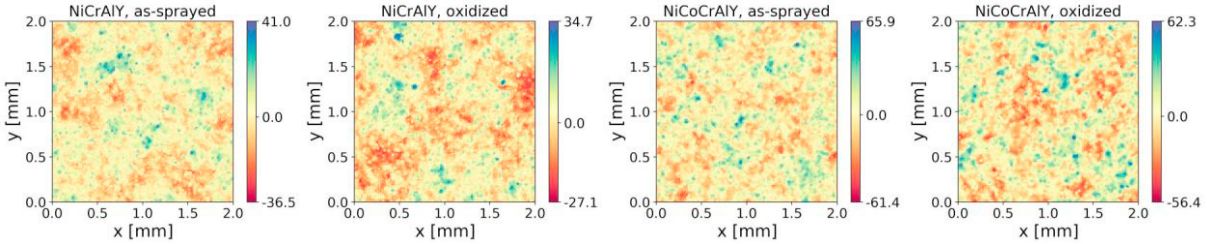

Fig. 2. Height maps (in microns) of as-sprayed and oxidized NiCrAlY and NiCoCrAlY bond-coats.

Table 2. Surface roughness parameters of as-sprayed and oxidized NiCrAlY and NiCoCrAlY bond-coats.

Parameter	NiCrAlY as-sprayed	NiCrAlY oxidized	NiCoCrAlY as-sprayed	NiCoCrAlY oxidized
S_a (μm)	7.3 ± 0.4	6.8 ± 0.5	12.6 ± 0.6	12.9 ± 0.5
S_q (μm)	9.3 ± 0.5	8.6 ± 0.5	15.8 ± 0.8	16.1 ± 0.4
Sk (-)	0.3 ± 0.1	0.3 ± 0.2	0.2 ± 0.1	0.1 ± 0.1
K (-)	0.3 ± 0.1	0.2 ± 0.0	0.1 ± 0.1	0.0 ± 0.1
R_S (-)	1.48 ± 0.01	1.23 ± 0.01	1.74 ± 0.02	1.54 ± 0.04

3.2. Thermal cycling

The results of FTC experiments are shown in Tab. 3, where the equivalent hot time (here the dwell time above the temperature of 1020 or 1120 °C) was calculated assuming the hot time of 22 min per cycle. In experiments with the top temperature of 1050 °C, the samples with the NiCoCrAlY bond-coat, which was rougher, endured less than half of the number of cycles to failure of samples with the flatter NiCrAlY bond-coat. This result may seem to be contradicting the deep-rooted fact that the torturous bond-coat surface generally results in superior performance when compared to the smooth one, but the two bond-coats simply are different materials and the NiCoCrAlY bond-coat

oxidizes more rapidly. Experiments with the top temperature of 1150 °C resulted in similar numbers of cycles to failure, nonetheless, the longer pre-oxidation time suggest that the samples with NiCrAlY bond-coat endured again, if only slightly, longer.

Table 3. The number of cycles to failure and the equivalent hot time (in parenthesis) in FTC test.

TBC system	#1 at 1050 °C	#2 at 1050 °C	#3 at 1150 °C
NiCrAlY–YSZ	3484	3762	306
(pre-oxidation 93 h)	(1278 h)	(1379 h)	(112 h)
NiCoCrAlY–YSZ	1274	1975	310
(pre-oxidation 66 h)	(467 h)	(724 h)	(114 h)

Microscopic observations revealed that the delamination cracks propagated mainly at the YSZ/TGO interface and in the YSZ layer in its close vicinity, the latter crack path being more frequent for experiments with the top temperature of 1150 °C. This result is consistent with outcomes of oxidation and thermal cycling study reported by Trunova et al. (2008) and it is caused by progressive accumulation of damage in the TGO layer and in the YSZ near it. The TGO layer after thermal cycling was more or less regular in undamaged regions, especially for the NiCrAlY bond-coat, and, again, was affected by the presence of pronounced interfacial irregularities and unmelted/partially-melted powder particles. Furthermore, growth of the TGO layer was also influenced by defects due to thermal cycling, Fig. 3. This mostly included cracks developed in the YSZ layer, particularly near the roughness peaks, and cracks propagating in the TGO layer, mainly at the peaks along its interfaces. Interestingly, the latter micromechanism that might be related to the delamination of the TGO layer from the bond-coat, which also induces tensile zones in the YSZ top-coat, see Slámečka et al. (2016) and Skalka et al. (2018), is dominant for the NiCoCrAlY coatings, where it manifests itself as multiple parallel cracks at the peaks, something practically not seen in the NiCrAlY coating. Similar damage of the NiCoCrAlY bond-coat was documented by Schlichting et al. (2003), Trunova et al. (2008) or, more recently, by Bolelli et al. (2019). It is believed that this multiple cracking is the main cause of lower endurance of TBCs with the NiCoCrAlY bond-coat found in this study and that this micromechanism requires further research.

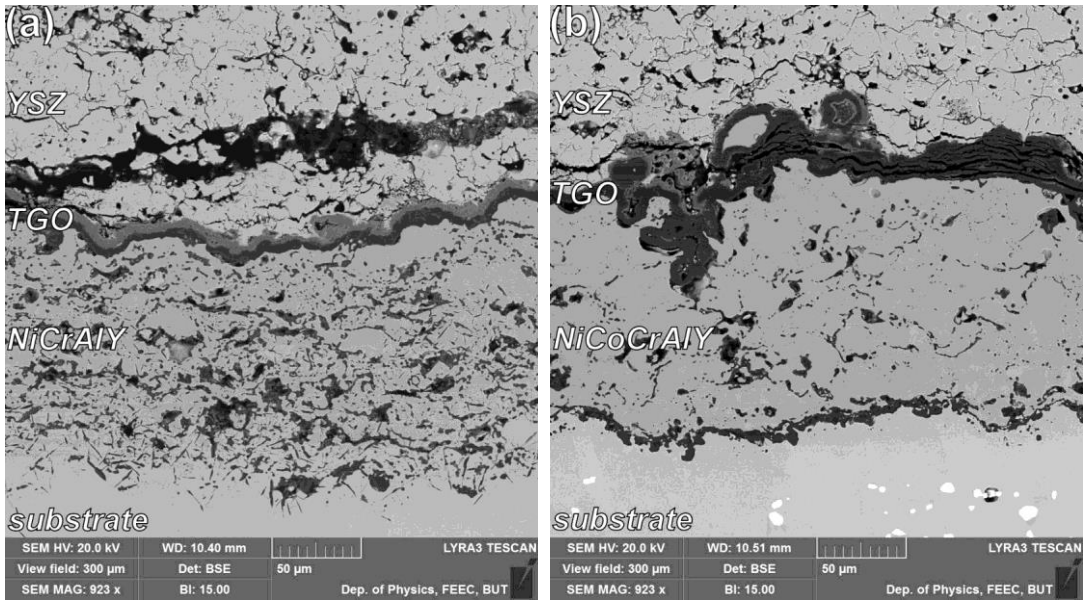

Fig. 3. (a) NiCrAlY–YSZ and (b) NiCoCrAlY–YSZ thermal barrier coatings after prolonged thermal cycling at 1050 °C.

4. Conclusions

This study dealt with thermal cycling of pre-oxidized NiCrAlY–YSZ and NiCoCrAlY–YSZ thermal barrier coatings. The NiCrAlY and NiCoCrAlY bond-coats presented different topographies, which was related to the different size of feedstock powders. The growth of the TGO layer was influenced by the presence of interfacial irregularities, unmelted or partially-melted feedstock powder particles, and defects induced by thermal cycling. Multiple parallel cracking of the TGO layer was important damage micromechanism for the NiCoCrAlY–YSZ thermal barrier coating system, which was responsible for its inferior performance.

Acknowledgements

The research was carried out under the project Research Center of Surface Treatment TE02000011 with financial support from the Technology Agency of the Czech Republic.

References

Dong, W.P., Sullivan, P.J., Stout, K.J., 1994. Comprehensive study of parameters for characterising three-dimensional surface topography III: Parameters for characterising amplitude and some functional properties. Wear 178, 45-60.

Bolelli, G, Righi, M.G., Mughal, M.Z., Moscatelli, R., Ligabue, O., Antolotti, N., Sebastiani, M., Lusvarghi, L., Bemporad, E., 2019. Damage progression in thermal barrier coating systems during thermal cycling: A nano-mechanical assessment. Materials and Design 166, 107615.

Eriksson, R., Sjöström, S., Brodin, H., Johansson, S., Östergren, L., Li, X.H., 2013. TBC bond coat-top coat interface roughness: Influence on fatigue life and modelling aspects. Surface & Coatings Technology 236, 230-238.

ISO 25178-2: 2012. Geometrical product specifications (GPS) – Surface texture: Areal – Part2: Terms, definitions and surface texture parameters.

Liu, D., Seraffon, M., Flewitt, P., Simms, N., Nicholls, J., Rickerby, D., 2013. Effect of substrate curvature on residual stresses and failure modes of an air plasma sprayed thermal barrier coating system. Journal of the European Ceramic Society 33, 3345-3357.

Padture, N.P., Gell, M., Jordan, E.H., 2002, Thermal barrier coatings for gas-turbine engine applications. Science 296, 280-284.

Schlichting, K.W., Padture, N.P., Jordan, E.H., Gell, M., 2003. Failure modes in plasma-sprayed thermal barrier coatings. Materials Science and Engineering A342, 120-130.

Skalka, P., Slámečka, K., Pokluda, J., Čelko, L., 2015. Stability of plasma-sprayed thermal barrier coatings: the role of the waviness of the bond coat and the thickness of the thermally grown oxide layer. Surface & Coatings Technology 274, 26-36.

Skalka, P., Slámečka, K., Pokluda, J., Čelko, L., 2018. Finite element simulation of stresses in a plasma-sprayed thermal barrier coating with a crack at the TGO/bond-coat interface. Surface & Coatings Technology 337, 321-334.

Slámečka, K., Čelko, L., Skalka, P., Pokluda, J., Němec, K., Juliš, M., Klakurková, L., Švejcar, J., 2015. Bending fatigue failure of atmospheric-plasma-sprayed CoNiCrAlY+YSZ thermal barrier coatings. International Journal of Fatigue 70, 186-195.

Slámečka, K., Skalka, P., Pokluda, J., Čelko, L., 2016. Finite element simulation of stresses in a plasma-sprayed thermal barrier coating with an irregular top-coat/bond-coat interface. Surface &Coatings Technology 304, 574-583.

Trunova, O., Beck, T., Herzog, R., Steinbrech, R., Singheiser, L., 2008. Damage mechanisms and lifetime behavior of plasma sprayed thermal barrier coating systems for gas turbines - Part I: Experiments. Surface & Coatings Technology 202, 5027-5032.

Vaßen, R., Kerhoff G., Stöver, D., 2001. Development of a micromechanical life prediction model for plasma sprayed thermal barrier coatings. Materials Science and Engineering A303, 100-109.

Zhang, X., Watanabe, M., Kuroda, S., 2013. Effects of processing conditions on the mechanical properties and deformation behaviors of plasma-sprayed thermal barrier coatings: Evaluation of residual stresses and mechanical properties of thermal barrier coatings on the basis of in situ curvature measurement under a wide range of spray parameters, Acta Materialia 61, 1037-1047.